Planet. Space Sci., Vol. 30, No. 5, pp. 457–461, 1982
Printed in Great Britain.

0032–0633/82/050457–05$03.00/0

LINE SHAPE OF THE NON-THERMAL 6300 Å O(^{1}D) EMISSION

G. A. SCHMITT, V. J. ABREU and P. B. HAYS
Space Physics Research Laboratory, The University of Michigan, Ann Arbor, MI 48109, U.S.A.

(*Received* 6 *October* 1981)

Abstract—The line shape of the non-thermal O(^{1}D) 6300 Å emission is calculated using the two population model of Schmitt, Abreu and Hays (*Planet. Space Sci.* **29**, 1095, 1981). The calculated line shapes simulate observations made from a space platform at different zenith angles and altitudes. The non-thermal line shapes observed at zenith angles other than the local vertical have been obtained by using the Addition theorem for spherical harmonics of a Legendre polynomial expansion of the non-thermal population distribution function.

I. INTRODUCTION

The atomic oxygen metastable state, O(^{1}D), is known to have a radiative lifetime of 110 s and is mainly produced in the night-time by dissociative recombination of O_2^+. These two factors are of importance in determining how transport and non-thermal processes affect the altitude profile of the 6300 Å emission and its Doppler line shape. The two principal physical processes involved here are diffusion and radiation of O(^{1}D) atoms before they are thermalized.

At night, the main source of O(^{1}D) atoms is the dissociative recombination of O_2^+:

$$O_2^+ + e \rightarrow O(^1D) + O(^3P, {}^1D, \text{ or } {}^1S). \quad (1)$$

The above reaction is exothermic with a net excess energy of 6.8 eV per recombination. This energy must be conserved either as excitation energy in the product atoms or as kinetic energy. Assuming that the excess energy is equally divided between the two fragments, the amount of kinetic energy (K.E.) can be 0.43, 1.55 or 2.0 eV per atom, depending on the electronic state (^{1}S, ^{1}D, ^{3}P) of the product oxygen atoms, respectively. It was shown by Hays and Walker (1966) that under these conditions the velocity distribution function of the atoms produced is given by

$$F(v) = \frac{v}{v_0}\sqrt{\left(\frac{\beta}{\pi}\right)}\{e^{-\beta(v-v_0)^2} - e^{-\beta(v+v_0)^2}\} \quad (2)$$

where $v_0 = \sqrt{(K \cdot \epsilon \cdot / m_O)}$, v is the atom's speed, $\beta = m_{O_2^+}/2\,kT$, m_O is the mass of an oxygen atom, $m_{O_2^+}$ is the mass of molecular oxygen, k is Boltzmann's constant, T is the temperature of the neutral atmosphere, and $F(v)$ is the isotropic velocity distribution function for the atoms created.

This distribution is characteristic of atoms which have not suffered a collision. Quenching collisions with N_2 and excitation exchange collisions with O(^{3}P) are important and must be considered. Schmitt *et al.* (1981) have developed a theoretical model in which O(^{1}D) atoms are separated into two distinct categories: non-thermal atoms which have suffered no collisions, and thermal particles which have undergone at least one excitation exchange with the O(^{3}P) population. The non-thermal atoms arise from the dissociative recombination of O_2^+. Sinks for this subpopulation include collisional quenching, emission of radiation (6300 Å) and thermalization by O(^{3}P). The second subpopulation is thermally distributed and consists of O(^{1}D) atoms thermalized by O(^{3}P). Sinks for the thermal subpopulation include collisional quenching and radiation. The two subpopulations are thus coupled by a thermalization cross-section which determines the loss and production in the non-thermal and thermal populations, respectively. Schmitt *et al.* (1981) have estimated the value of the thermalziation cross-section to range from 1.0 to 2.0×10^{-15} cm^2, from observation of the non-thermal 6300 Å emission at high altitude. This paper will consider the theoretical line shape of the O(^{1}D) red line emission derived from the two-population model by Schmitt *et al.* (1981). Simulated observations of red line profiles at arbitrary zenith angles from a space platform will be presented. These calculations are relevant in view of the line shape measurements being carried out with the Fabry–Perot interferometer (Hays *et al.*, 1981) on board the Dynamics Explorer satellite.

II. NON-THERMAL SPECTRAL LINE SHAPE

The following assumptions will be made in the analysis that follows: (1) the velocity of each fragment atom is constant even in the presence of the Earth gravitational field; (2) elastic collisions have no effect on the speed and (3) non-thermal $O(^1D)$ atoms are thermalized by single collisions [excitation exchange with $O(^3P)$].

The probability that oxygen atoms created at altitude z and zenith angle ϕ will be neither quenched nor thermalized at altitude z_0 is given by (Schmitt *et al.*, 1981)

$$S(z, z_0) = \exp\left[-\Delta\tau(z, z_0)/\mu\right] \tag{3}$$

where

$$\Delta\tau(z, z_0) = \sigma_0 N_0(z, z_0) + \sigma_Q N_{N_2}(z, z_0) + \frac{A_{^1D}(z - z_0)}{|\mathbf{v}|} \tag{4}$$

$$N_i(z, z_0) = \int_z^{z_0} \eta_i(z')\,dz' \tag{5}$$

$\mu = \cos\phi$
η_i = number density of the ith species
σ_0 = thermalization cross-section
σ_Q = cross-section for quenching
$A_{^1D}$ = spontaneous emission rate for $O(^1D)$ atoms
$\mathbf{v}$ = velocity of the product oxygen atom.

The terms in equation (4) include the probabilities of thermalization in one collision by excitation exchange with $O(^3P)$, quenching by N_2 and spontaneous radiation at 6300 Å, respectively.

The flux of non-thermal $O(^1D)$ atoms in an element of solid angle $d\Omega$ is

$$F(z, z_0) = P(z)\frac{d\Omega}{4\pi}e^{-\Delta\tau/\mu}\,dz \tag{6}$$

where $P(z)$, the rate of production of $O(^1D)$ atoms by dissociative recombination, is given by

$$P(z) = \beta_{^1D}[O_2^+]n_e \tag{7}$$

where $\beta_{^1D}$ is the specific recombination rate, $[O_2^+]$ is the molecular oxygen ion number density, and n_e is the electron number density.

The number of photons emitted at z_0 by $O(^1D)$ atoms created with a vertical component of velocity between w, $w + dw$ is

$$\eta = \frac{A_{^1D}}{4\pi v_0 w}P(z)\,e^{-\Delta\tau/\mu}\,dz\,d\theta\,dw \tag{8}$$

where $w = -v_0\cos\phi$.

The line profile of this non-thermal emission viewed along a vertical line of sight is easily derived since the wavelength of the emission is directly related to the vertical component of velocity by

$$\lambda - \lambda_0 = \frac{\lambda_0 w}{c}, \tag{9}$$

where λ_0 is the wavelength of the emission in the rest frame of the emitting oxygen atom, and c is the speed of light. Integrating over the production region and making use of equation (9) one obtains the following expressions for the spectral line shapes at altitude z_0 when viewed vertically upward,

$$\frac{d\eta}{d\lambda} = \frac{A_{^1D}}{4\pi v_0(\lambda - \lambda_0)}\int_0^{z_0}\int_0^{2\pi} P(z)\,e^{-(v_0\Delta\tau\lambda_0/c(\lambda_0-\lambda))}\,d\theta\,dz \qquad \lambda > \lambda_0$$

$$\frac{d\eta}{d\lambda} = \frac{A_{^1D}}{4\pi v_0(\lambda - \lambda_0)}\int_{z_0}^{\infty}\int_0^{2\pi} P(z)\,e^{-(v_0\Delta\tau\lambda_0/c(\lambda-\lambda_0))}\,d\theta\,dz \qquad \lambda < \lambda_0. \tag{10}$$

These expressions are easily evaluated numerically and can be extended to the case where the initial production of $O(^1D)$ atoms has the velocity distribution $F(v)$ given by equation (2). The extension to a distribution of initial velocities requires only an integration over the initial velocity weighted by the distribution function.

III. NON-VERTICAL LINES OF SIGHT OBSERVATIONS

Observations of the red line emission from a high altitude space platform include contribution from different altitudes along the line of sight. At each altitude the line of sight is displaced from the local vertical by an angle χ. The line shape of the thermally distributed population can easily be obtained at each altitude by calculating the component of the vertical diffusion velocity along the line of sight and effecting the appropriate wavelength shift. The diffusion velocity is obtained by a solution of the diffusion equation as shown by Schmitt *et al.* (1981). The proper treatment of the non-thermal case, however, requires some care. The non-thermal profile for an arbitrary line of sight can be calculated, given the Legendre polynomial expansion about the local vertical of the distribution function of the non-thermal population.

Consider a function $f(\chi)$ in a spherical coordinate system (ϕ_1, θ_1) where χ, defined by

$$\cos\chi = \cos\phi_1\cos\phi_2 + \sin\phi_1\sin\phi_2\cos\theta_1, \tag{11}$$

is the angle between the vector (ϕ_1, θ_1) and a new reference system (ϕ_2, θ_2). A Legendre polynomial expansion of $f(\chi)$, and a subsequent application of the Addition theorem for spherical harmonics yields

$$f(\chi) = \sum_{n=0}^{\infty} A_n \Big[P_n(\cos\phi_1)P_n(\cos\phi_2) \tag{12}$$
$$+2\sum_{i=1}^{n}\frac{(n-i)!}{(n+i)!}\sin^i\phi_1\sin^i\phi_2\,P_n^{(i)}(\phi_1)P_n^{(i)}(\phi_2)\cos(i\theta_1)\Big],$$

where we have arbitrarily set the azimuth angle θ_2 equal to zero. Equation (10) is of the form,

$$\frac{d\eta}{d\lambda} = \frac{A_{^1D}}{v_0}\int_0^{2\pi} f(\chi)\,d\theta_1, \tag{13}$$

where $f(\chi)$ has units of photons cm^{-3}s^{-1}sr^{-1}.

The substitution of equation (12) for $f(\chi)$ and effecting the integral in equation (13) yields

$$\frac{d\eta}{d\lambda} = \frac{2\pi A_{^1D}}{v_0}\sum_{n=0}^{\infty} A_nP_n(\cos\phi_1)P_n(\cos\phi_2). \tag{14}$$

Here ϕ_2 is the angle between the line of sight and the local vertical, while $\cos\phi_1 = (\lambda - \lambda_0)c/\lambda_0 v_0$. Equation (14) allows one to calculate the non-thermal line shape when viewed at any angle ϕ_2 with the local vertical.

IV. LINE SHAPE SIMULATIONS

The theory just presented will be used to calculate 6300 Å emission line profiles which simulate measurements from a space platform along different lines of sight. Each simulated measurement consists of the sum of the line shapes at each point along the line of sight of the observation. The non-thermal line shape contribution at each point along the path of observation has been obtained using equation (14). The simulations that follow have used the MSIS neutral atmosphere model (Hedin *et al.*, 1977a, b) and an electron density profile obtained at Millstone Hill on March 1973 at 20:00 hr. Other parameters used in the calculation are shown in Table 1.

Figure 1 shows the theoretical non-thermal line shape as viewed from a space platform at 500 km altitude at different zenith angles. The observed cut-off in the line shape at ±0.1259 Å is due to the fact that we have chosen 3.1 eV to be the constant velocity of an O(^{1}D) atom. When the zenith angle is less than 90° (looking up) most of the observed non-thermal emission is from O(^{1}D) atoms produced below the altitude of the observing platform and moving away from it (red shifted emission). At a zenith angle equal to 90° the line shape is symmetric about 6300 Å, while for zenith angles greater than 90° (looking downward) the blue shifted emission is slightly enhanced. Figures 2–4

TABLE 1

$\sigma_Q = 1.38\times10^{-16}$ cm^2.
$\sigma_0 = 1.5\times10^{-15}$ cm^2.
$A_{^1D} = 0.0068$ s^{-1}.
$\beta_{^1D} = 2.1\times10^{-7}(300/T)^{0.55}$ cm^3 s^{-1}.
Peak electron density $= 4.0\times10^5$ cm^{-3}.

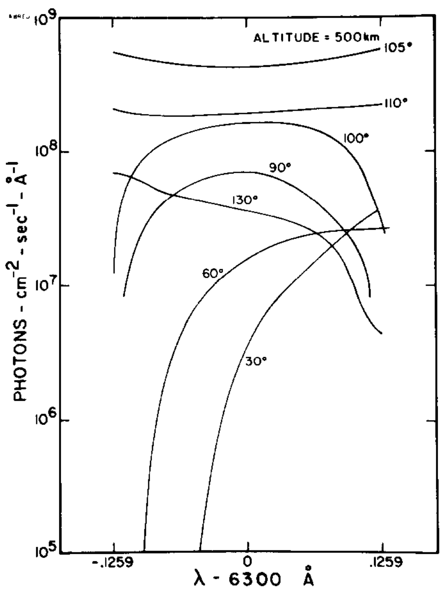

FIG. 1. THEORETICAL NON-THERMAL LINE SHAPE AS VIEWED FROM A SPACE PLATFORM AT 500 km ALTITUDE AT DIFFERENT ZENITH ANGLES.

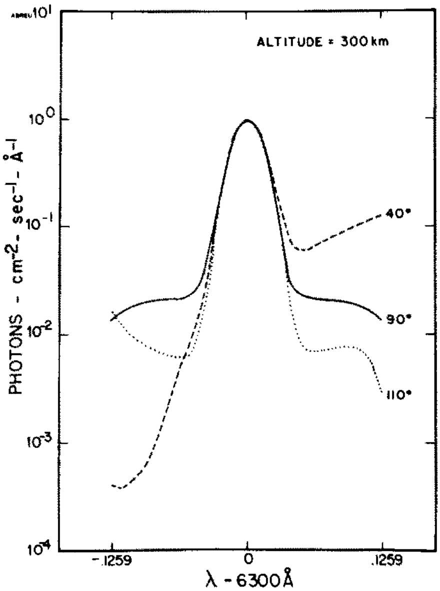

FIG. 2. COMBINED LINE SHAPES (THERMAL PLUS NON-THERMAL) NORMALIZED TO THE 6300 Å INTENSITY AS VIEWED FROM A SPACE PLATFORM AT 300 km ALTITUDE AND SELECTED ZENITH ANGLES.

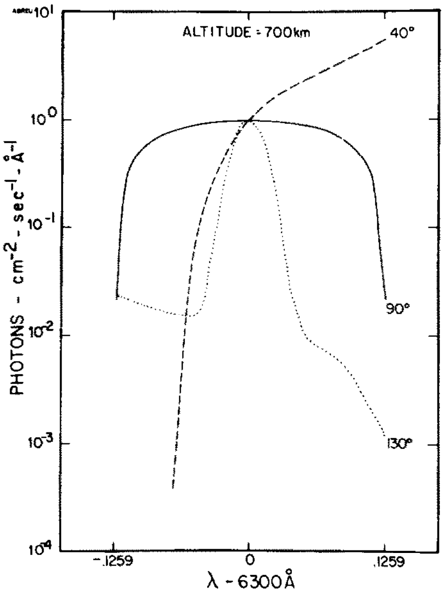

FIG. 4. SAME AS FIG. 2, EXCEPT THE ALTITUDE OF OBSERVATIONS IS 700 km.

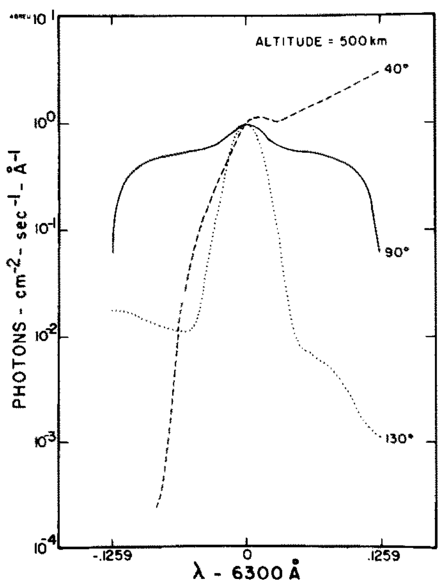

FIG. 3. SAME AS FIG. 2, EXCEPT THE ALTITUDE OF OBSERVATIONS IS 500 km.

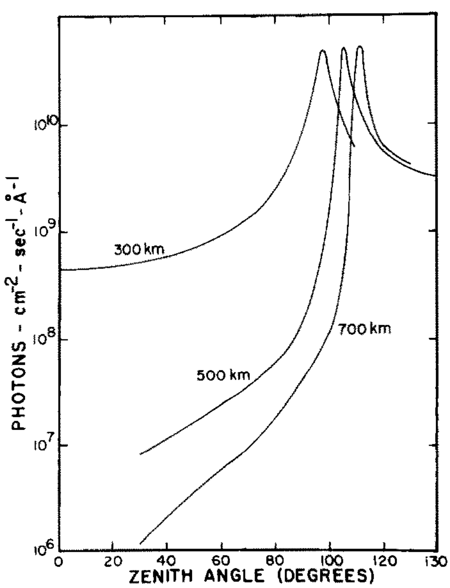

FIG. 5. THE CALCULATED INTENSITY AT 6300 Å AS A FUNCTION OF ZENITH ANGLE FOR ALTITUDES EQUAL TO 300, 500 AND 700 km.

show the combined line shapes (thermal plus non-thermal) as viewed from 300, 500 and 700 km, respectively. The line shapes have been normalized to the intensity at 6300Å. As the observing altitude decreases, the thermal features become more pronounced. For example, at 500 km when looking at a zenith angle of 40° (see Fig. 3) the thermal contribution to the line shape appears as a small swelling embedded in the non-thermal line. The calculated intensity at 6300 Å is shown in Fig. 5 as a function of zenith angle of observation for three altitudes. The units are photons $cm^{-2}\,s^{-1}\,Å^{-1}$.

Preliminary considerations of the instrument function of the Fabry–Perot interferometer (FPI) on board the Dynamics Explorer satellite indicate that this instrument will be capable of measuring the non-thermal component of the 6300 Å emission. The theory just presented will be used to interpret the 6300 Å line profiles measured by the FPI. This work is in progress.

Acknowledgement—This work was supported by NASA Grant NAS5-23006 and NSF Grant ATM80-05359.

REFERENCES

Hays, P. B. and Walker, J. C. G. (1966). Doppler profiles of the 5577 Å airglow. *Planet. Space Sci.* **14**, 1331.

Hays, P. B., Killeen, T. L. and Kennedy, B. C. (1981). The Fabry–Perot interferometer on Dynamics Explorer. *Space Sci. Instrum.* **5**, 345.

Hedin, A. E., Salah, J. E., Evans, J. V., Reber, C. A., Newton, G. P. Spencer, N. W. Kayser, D. C., Alcayde, D., Bauer, P., Cogger, L. L. and McClure, J. P. (1977a). A global thermospheric model based on mass spectrometer and incoherent scatter data MSIS 1: N_2 density and temperature. *J. geophys. Res.* **82**, 2139.

Hedin, A. E., Reber, C. A., Newton, G. P., Spencer, N. W., Brinton, H. C. and Mayr, H. G. (1977b). A global thermospheric model based on mass spectrometer and incoherent scatter data MSIS 2: Composition. *J. geophys. Res.* **82**, 2184.

Schmitt, G. A., Abreu, V. J. and Hays, P. B. (1981). Non-thermal (O(¹D) produced by dissociative recombination O_2^+: A theoretical model and observational results. *Planet. Space Sci.* **29**, 1095.